Bidirectional Converter with High Frequency Isolation Feasible to Solid State Transformer Applications

Luan Carlos Mazza, Demercil Oliveira, Fernando Antunes, Antonio Dias,
Jose Cleomon da Silva and Alisson Freitas
FEDERAL UNIVERSITY OF CEARA
Centro de Tecnologia - Campus do Pici, Bl. 705
Fortaleza-CE, Brazil
Phone: +55 (85) 3366-9581
Fax: +55 (85) 3366-9574
Email: luanmazza@ifce.edu.br
URL: http://www.dee.ufc.br

Acknowledgments

The authors acknowledge the GPEC by the availability of laboratory and materials.

Keywords

≪AC-DC Converter≫, ≪NPC≫, ≪Phase shift≫, ≪Solid State Transformer≫, ≪ZVS≫.

Abstract

This paper presents a new three-port ac-dc converter topology based on the bidirectional version of the three-state switching cell (3SSC) and neutral point clamped (NPC) with Dual Active Bridge (DAB) feasible to interconnect an AC link, a DC link and photovoltaic panels. The three port converter operates as solid state transformer (SST). It the primary side switches voltage and current stresses are reduced due to NPC and 3SSC characteristics. Some operating ranges presented Zero Voltage Switching (ZVS). Modulation strategy and control are presented. For the drive control was implemented five control loops: PFC (Power Factor Correction); full voltage and balancing voltages acroos port 2 capacitors; magnetization current and voltage on port 3. A 33.33 kW converter with the peak value of the AC voltage is 9.35 kV and DC voltage at port 3 is 800 V with a DC bus voltage at port 2 of 22 kV has been simulated. A comparative loss studies with other converter topologies is also made. The proposed topology presented efficiency of 97.2%.

Introduction

The conventional power transformers are widely used in electrical energy distribution systems for voltage conversion and galvanic isolation. Often, power electronics based systems are necessary to address the power quality issues. Also, there is a growing demand for the integration of distributed renewable generation sources into the distribution grid. Therefore, the creation of a device que integrates an electronic circuit with isolation ability to distribution systems was necessary. Solid state transformers are the new trend for power distribution systems, because with them the exchange of large power transformers is possible for smaller systems, more efficiency and more capabilities.

State Solid Transformer (SST) exhibits high power density, controlled power factor, bidirectional power flow, voltage sag compensation, integration of distributed energy sources, possible to minimize size, weight and volume of the whole system [1], [2]. The creation of new topologies [3], [4], [5] the advancement in the development of semiconductor able to support high voltages, currents and frequencies, as

well as the development of new magnetic designs [6] has made the SST increasingly become a reality. SST model is presented in Fig. 1.

Usually, multilevel converters were being used in motor drives, in the meantime, due to advances in techniques and processes in manufacturing semiconductor devices, the use of this equipment in systems that operate at medium and high powers are growing [7]. Monophasic converters five levels based on the multi-state switching cell with the neutral-point clamped (5-NPC), one of the types of voltage-fed converters, present advantages like the fact reduce the losses while driving and switching of the semiconductor switches, reduce the amount of harmonics in the output waveform and own reduced size and volume of magnetic components [7].

The topology proposed in this work consists of a single phase converter five-level with dual neutral point clamped based on the Three State Switching Cell (D3S).

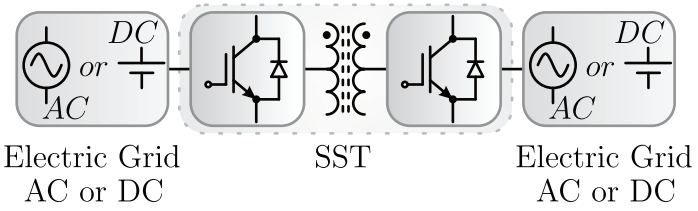

Fig. 1: SST model.

Proposed system

The proposed system is presented in Fig. 2. Basically the converter has to operate as a rectifier, fulfilling the function of processing power from the AC link (peak value is 9.35 kV) to feed a DC link (800 V).

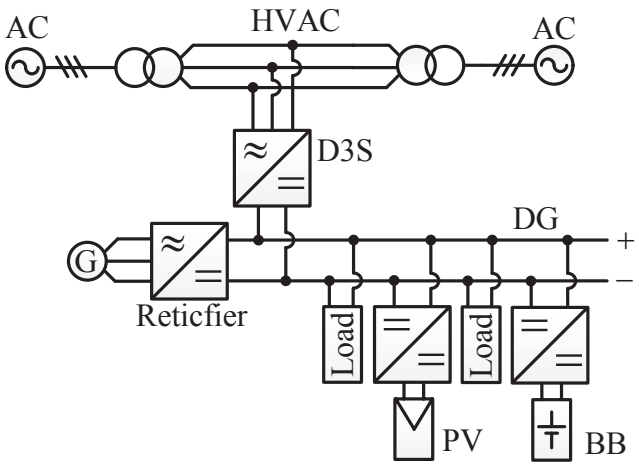

Fig. 2: Proposed system application.

Design and description of topology

Converter combines the three state switching cell (3SSC) based in [8] with two three-level neutral point clamped (DNPC) converter topology [9] and Dual Active Bridge (DAB) has characteristics [10]. Converter has three ports (behaves as input or output for the power flow), characteristics having DC-link in two ports and AC-link in a port.

The design of the structure is based in [11]. The original topology operated with DC-DC features, but the D3S operates on AC-DC and has the primary two arms with three-level switches, it can be seen in Fig. 3(a). Three-phase version of the proposed topology is presented in Fig. 4.

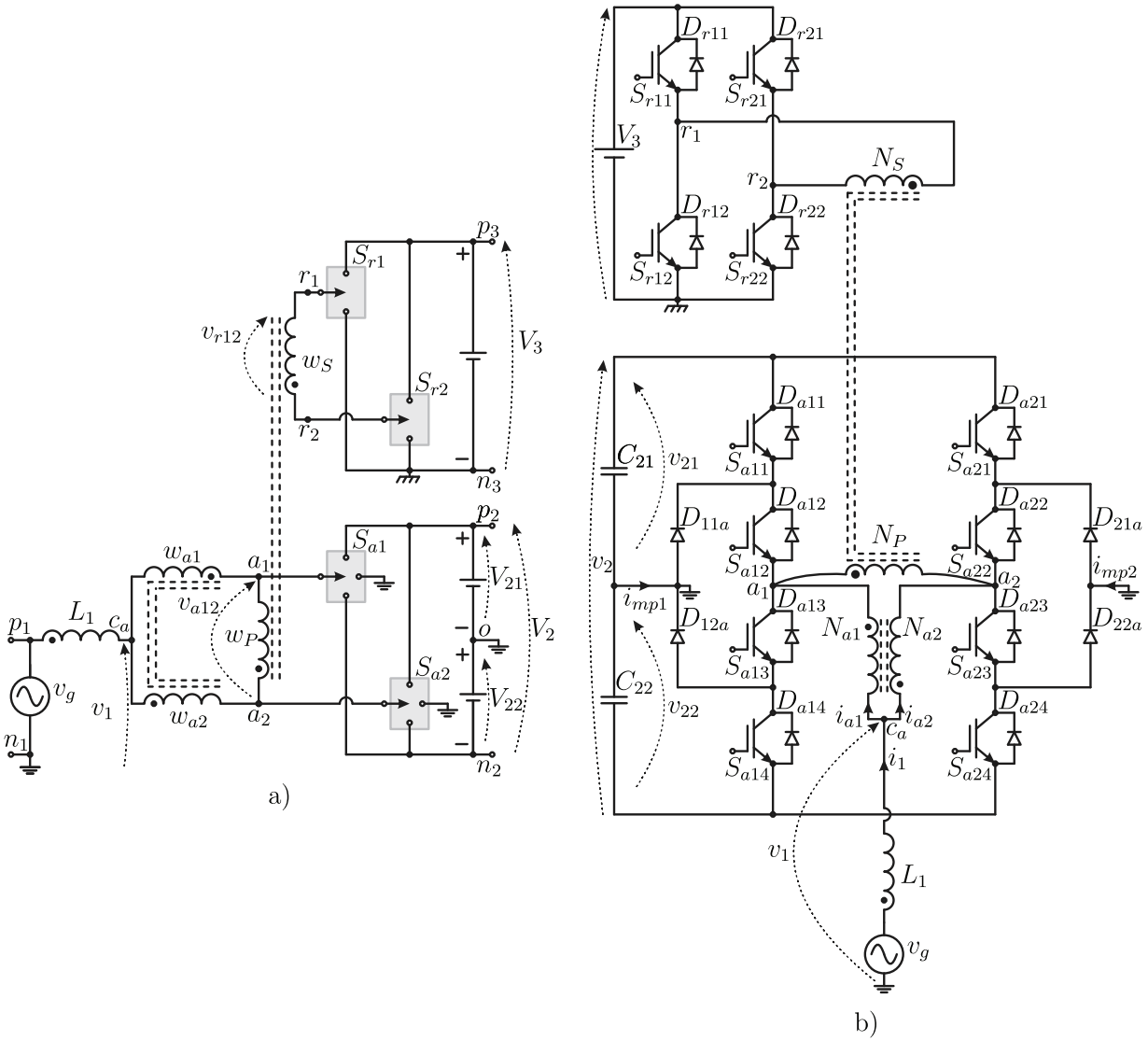

Fig. 3: Proposed topology: (a) Generic and (b) Single-phase version (D3S).

Fig. 3(b) shows the proposed converter, here called D3S. The primary switches in the converter are subjected to half of the link voltage due to the port 2 of the three level NPC, this reduces the voltage stress on the switches, thus being able to operate with lower voltage switches. In configuration presented, the current also divides the switches of the two windings of the autotransformer, thereby decreasing the stress current in the switches.

The instantaneous value of the multilevel voltage v_1 and transformer primary v_{a12} are given by (1) and (2), respectively.

$$v_1 = \frac{v_{a10} + v_{a20}}{2} \tag{1}$$

$$v_{a12} = v_{a10} - v_{a20} \tag{2}$$

Where v_{a10} and v_{a20} are the instantaneous values of the voltage produced in the primary arms (NPC).

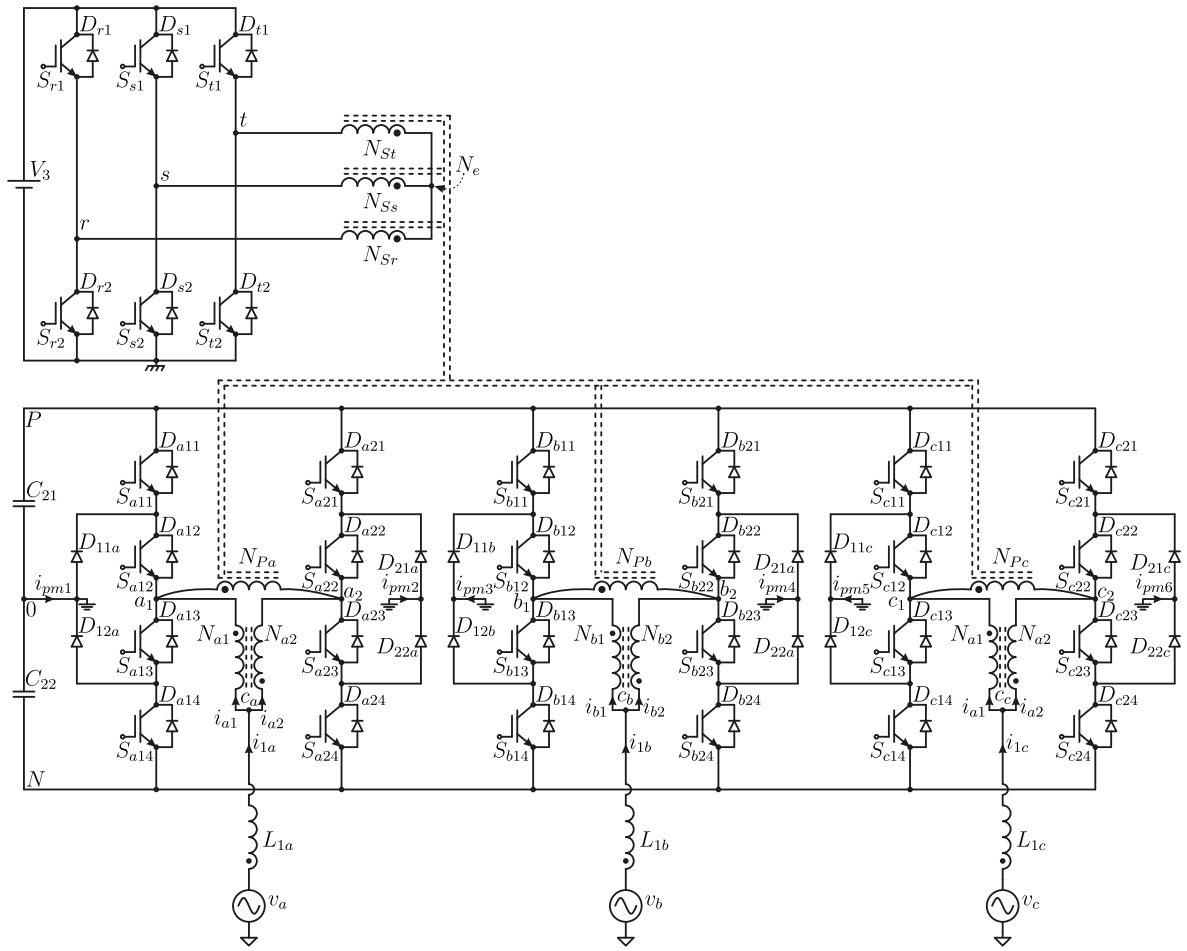

Fig. 4: Three-phase version of the proposed topology.

Modulation strategy

The modulation strategy is based carriers. The comparison between the modulation function, in primary (m_p) and secondary (m_s) side, and the carriers generate the switching functions (3), where for a generic switch is considered $x, j \in \{1,2\}$ and $y \in \{1,\ldots,4\}$ in primary side. The generating circuit of the switching signals shown in Fig. 5(a), while presents waveforms of modulating signals from the primary and secondary side in Fig. 5(b). For the primary side, when $m_p \geq c_{axj}$ then $d_{axy} = 1$, in the other case $d_{axy} = 0$.

$$d_{axy} = \begin{cases} 1 \Leftrightarrow m_p(\theta_g) \geq c_{axj}(\theta_{axj}) \\ 0 \Leftrightarrow m_p(\theta_g) < c_{axj}(\theta_{axj}) \end{cases} \tag{3}$$

In secondary side, comparison logic is the same as the primary side. The switching functions are given by (4), where $x, j \in \{1,2\}$.

$$d_{rxj} = \begin{cases} 1 \Leftrightarrow m_p(\theta_g) \geq c_{rxj}(\theta_{rxj}) \\ 0 \Leftrightarrow m_p(\theta_g) < c_{rxj}(\theta_{rxj}) \end{cases} \tag{4}$$

The modulation functions are given by

$$m_p = M\cos(\omega_g t) \tag{5}$$

$$m_s = 2M\left|\cos(\omega_g t)\right| - 1. \tag{6}$$

where $\omega_g = 2\pi f_g$ and f_g is grid frequency. The Variable M is modulation index (7). Another important

relationship is the M_f frequency modulation index which is given by (8).

$$M = \frac{2\hat{V}_g}{V_2} \tag{7}$$

$$M_f = \frac{f_s}{f_g} \tag{8}$$

where $\hat{V}_g$ is peak value grid voltage, V_2 is DC link voltage in port 2, $\omega_g = 2\pi f_g$ and f_s is switching frequency.

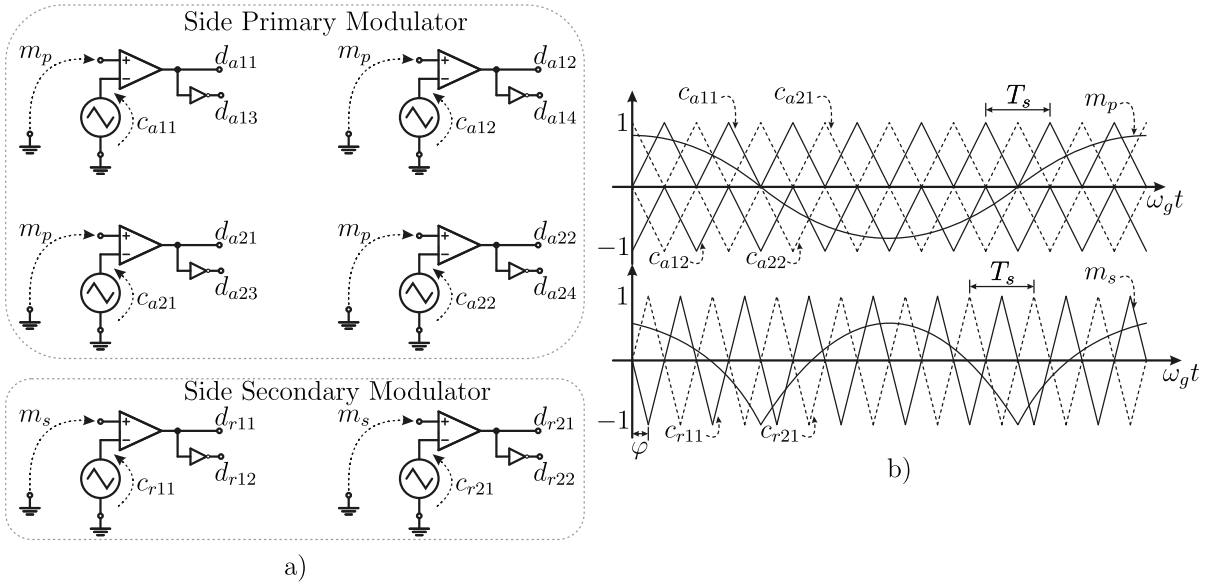

Fig. 5: Modulation strategy: (a) Circuit modulator of the primary and secondary sides and (b) Waveforms of signals modulators and carriers.

Control strategy

The converter control strategy is responsible for five control loops: PFC, full voltage and balancing tensions in port capacitors 2, magnetization current and voltage on port 3. Block diagram of the used control strategy in proposed topology is presented in Fig. 6.

The PFC and control voltage on port 2 is performed through the control of average current. In this strategy were inserted to voltage balancing loop on port 2 and control of the magnetizing current. The gains of the voltage sensors and drive current are by H_{v2}, H_{v3}, H_{i1} and H_{im}. All compensators ($C_{v2}(s)$, $C_{v3}(s)$, $C_{i1}(s)$ and $C_{im}(s)$) are implemented PI (proportional-integral). The phase shift control strategy is responsible for controlling the voltage at port 3 (V_3).

Simulation results

This section is presented simulation results of the converter proposed. Main simulation specifications and parameters are presented in Table I.

The Fig. 7 shows the result of simulation current drained the mains. It can be seen that the control was effective because the Power Factor (PF) was 0.998 and the Total Harmonic Distortion (THD) of the mains was drained of 3.18%. Fig. 7 shows also the detail of the drained current the mains between 500ms and 600ms.

It is noted that the control maintaining voltage and current substantially in phase. Fig. 8 shows the waveforms of voltage on capacitors C_{21} and C_{22}. . Fig. 9(a) show the transformer magnetizing current and is shown in the Fig. 9(b) the voltage at port 3.

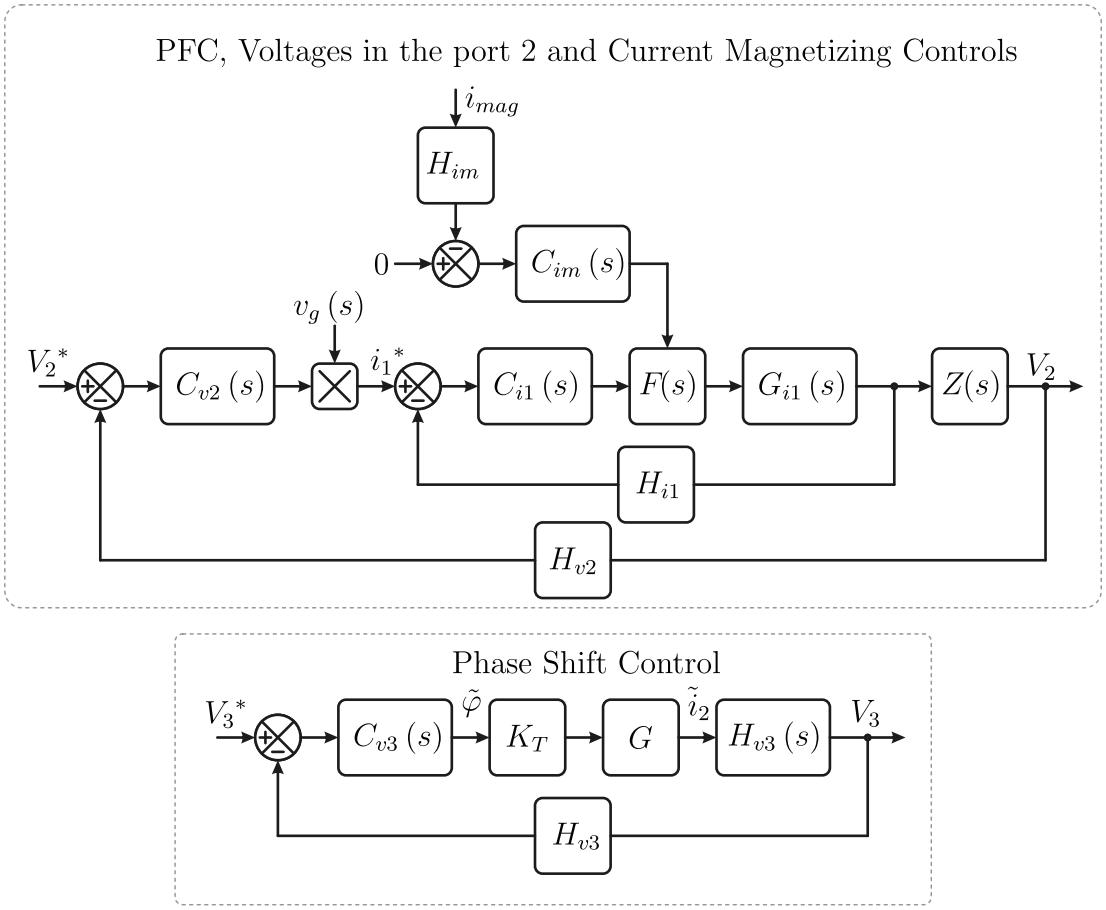

Fig. 6: Block diagram of the used control strategy in proposed topology.

Table I: Main simulation specifications and parameters

Parameters	Specifications
Power, Port 3 (P_3)	33.33 kW
Peak Value Voltage Phase, Grid ($\hat{V}_g$)	9.35 kV
Voltage, Port 2 (V_2)	22 kV
Voltage, Port 3 (V_3)	800 V
Inductance, Port 1 (L_1)	100 mH
Capacitances, Port 2 (C_{21} and C_{22})	10 μF
Capacitance, Port 3 (C_3)	470 μF
Transformer Turns Ratio (t_1)	13.75
Auto-Transformer Turns Ratio (at_1)	1

Comparative losses study

Comparative losses study are presented considering in the transformer a frequency of 10 kHz, ac grid ratings of 13.8kV/60Hz, dc link voltage of 800V and output power of 100kW. For the comparative study of losses all calculations and simulations were carried out for three-phase arrangements including the proposed topology.

To perform the comparative losses, the converter studied in this article will be bought with three converters. The first converter (converter A) to be analyzed is shown in [4]. The VSI has a Multilevel convertor studied AC-AC, where the implementation of a LC filter to correct the ripple in input current was necessary. Moreover, it was seen that the converter has a ZVS switching for a bidirectional flow. This feature has proven very interesting considering high switching frequency.

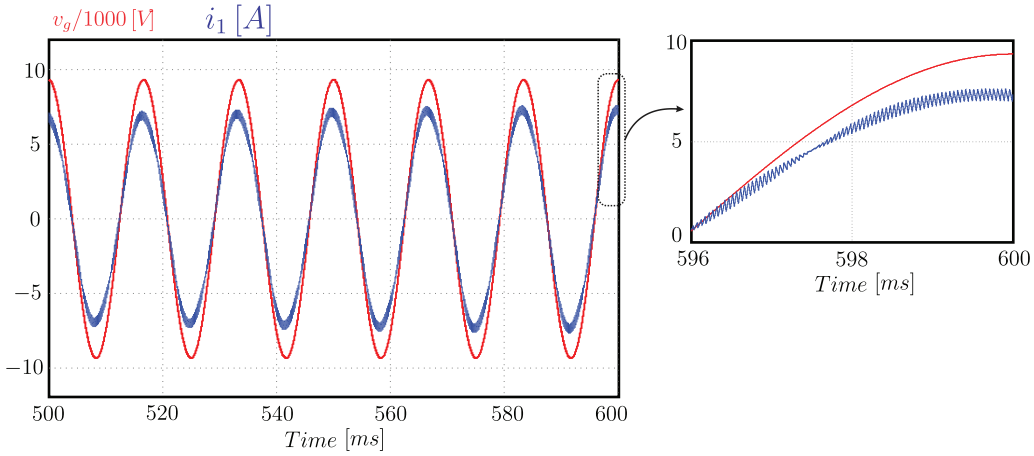

Fig. 7: Waveforms of voltage and current drained from the grid.

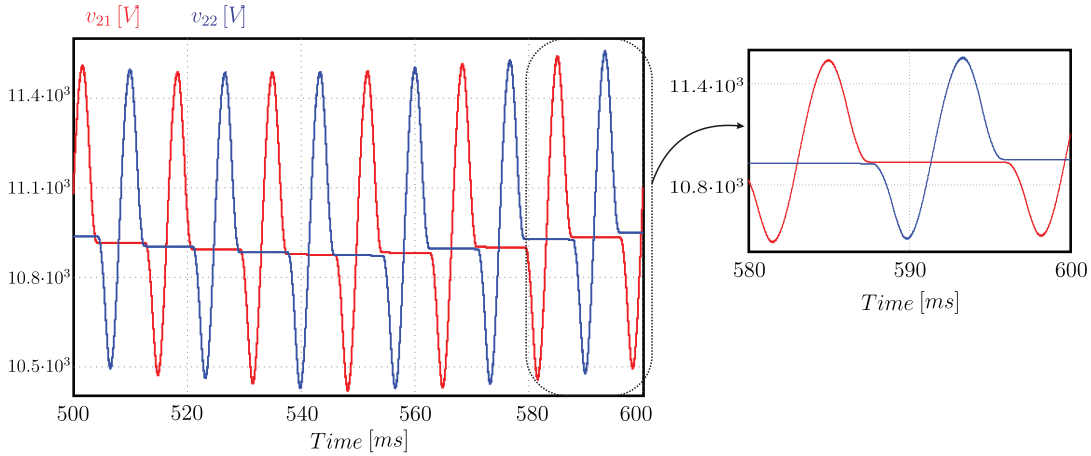

Fig. 8: Waveforms of voltage and current drained from the grid.

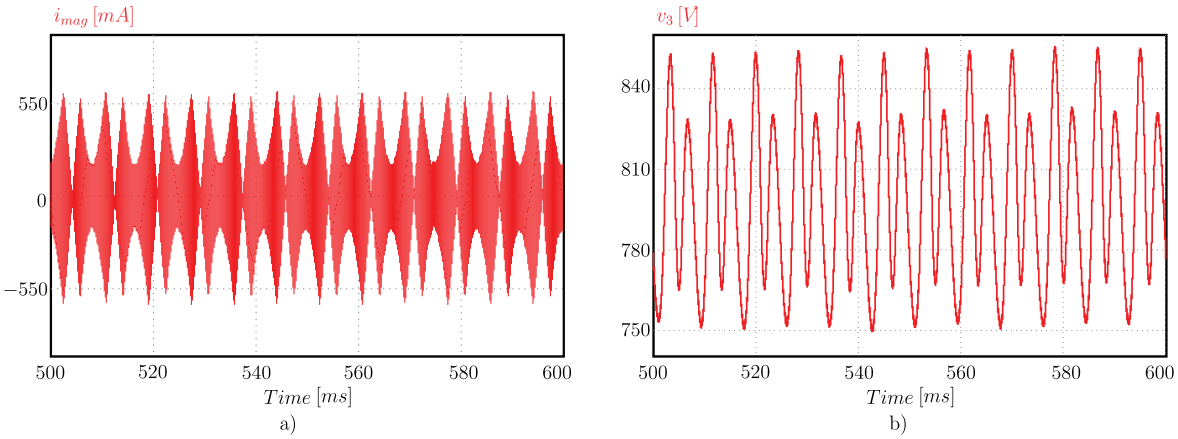

Fig. 9: waveforms of: (a) Magnetizing current and (b) Voltage in the port 3.

Another important feature of the AC-AC converter is the high value of the ripple currents through switch and the primary voltage of the medium-frequency transformer, requiring the implementation of a snubber to reduce ripples. The converter has obtained satisfactory operation for a power of 100kW, but presented in a high open-loop reactive flow. After the medium frequency transformer has a PWM rectifier used in charging the battery bank. . Like the AC-AC converter, the rectifier PWM switching is also ZVS.

The second converter (converter B) is the modular cascaded h-bridge based on Solid State Transformer presented in [5]. The first stage is based on an AC/DC converter with H-bridge cell multilevel converter. In the DC/DC stage conversion is presented the Dual Active Bridge (DAB) converter, which is characterized by using a transformer operating at high frequency in order to adjust the voltage level between two DC levels, in general the high voltage level corresponds to the distribution voltage and low voltage level is the voltage in the end user consumption level.

Finally, the last conversion stage is present in a DC/AC converter which can be connected independently of each module, or may be connected to form another multilevel converter.

The third converter (converter C) is a three-stage converter [12], [13] but in this paper only the two first stages are studied. The first stage is an AC/DC converter composed by a 3-Level Neutral Point Clamped Converter (3-L NPC), where an LCL filter is use to search a compromise between eliminate switching ripple at input current (13.8kV) and reduce the filter size [14]. The second stage is a DC/DC converter composed by a three-phase Y:Y/ DAB converter [15]. In this topology a 3-L NPC converter is connect to primary star-winding and 2 two-level converters are connected to two secondary windings in star-delta of the Media Frequency Transformer (MFT).

The two-level converters of the Low Voltage (LV) side are in 30 phase-shift so that they produce synchronous fundamental flux. Because of this a higher order odd-harmonics are cancelled-out due to 150 and 210 phase difference. Then these harmonic voltages not excite transformer EMF resulting in a nearly sinusoidal currents in the Medium Voltage (MV) side of the transformer. However the two-level sides have a harmonic currents circulating between them [15], [16]. The comparative losses study is presented in Table II.

Table II: Comparative losses in the studied topologies

Topology	A	B	C	Proposed
Conduction losses	1.22 kW	1.05 kW	1.37 kW	1.11 kW
Commutation losses	0.98 kW	2.2 kW	2.49 kW	1.72 kW
Total losses	2.2 kW	3.25 kW	3.86 kW	2.83 kW
Efficiency	97.8%	96.7%	96.1%	97.2%
First harmonic order (i_1)	f_s	f_s	f_s	$2f_s$
Primary switches number	24	36	24	24

As can be seen in Table II, the efficiency of the proposed topology is 97.2% with a difference to the 0.6% to the best result. The first harmonic of the input voltage is the same on the topologies A, B and C and has a frequency equal to the switching frequency, while the proposed topology presents a first harmonic of twice the switching frequency. About the number of switches used in the primary side of the MFT: the proposed topology use the same number of topologies A and C, while a topology C uses a 33% greater number of switches.

Conclusion

This paper has proposed a dual NPC based on three state switching cell, with characteristics DAB. The main advantage of the topology is a voltage reduction across the power switches. Also, high power factor (0.998) and low THD (3.18%) of the current drained from the AC grid are main advantages of the proposed converter. The converter also features high voltage gain and buck or boost characteristic in port 3.

References

[1] L. Yang, T. Zhao, J.Wang, and A.Q.Huang, Design and analysis of a 270kW five-level dc/dc converter for solid state transformer using 10kV SiC power devices, in Proc. IEEE Power Electronics Specialist Conference, June 2007, pp.245-251.

[2] A. Abedini, and T. Lipo, A novel topology of solid state transformer, in Proc. Power Electronic & Drive Systems and Technologies Conference (PEDSTC 10), 2010, pp.101-105.

[3] S. Falcones, X. Mao, and R. Ayyanar, Topology comparison for solid state transformer implementation, in Proc. IEEE Power Energy Soc. Conf., 2010, pp1-8.

[4] Oliveira, Demercil S.; Honorio, Dalton de A.; Barreto, Luiz Henrique S.C.; Praca, Paulo P., "A Single-Stage AC-DC Modular Cascaded Multilevel Converter Feasible to SST Applications," PCIM Europe 2015; International Exhibition and Conference for Power Electronics, Intelligent Motion, Renewable Energy and Energy Management; Proceedings of , vol., no., pp.1,8, 19-20 May 2015.

[5] Garcia Montoya, R.J.; Mallela, A.; Balda, J.C., "An evaluation of selected solid-state transformer topologies for electric distribution systems," Applied Power Electronics Conference and Exposition (APEC), 2015 IEEE , vol., no., pp.1022,1029, 15-19 March 2015.

[6] Y. Du, S. Baek, S. Bhattacharya, and A. Q. Huang, High-voltage high frequency transformer design for a 7.2kV to 120V/240V 20kVA solid state transformer, in Proc. IEEE Industrial Electronics Society Conference (IECON), Nov 2010, pp. 493498.

[7] Firouz, Y.; Bina, M.T. and Eskandari, B., Efficiency of three-level neutral-point clamped converters: analysis and experimental validation of power losses, thermal modelling and lifetime prediction, in IET Power Electronics, 2014, Vol. 7, pp. 209 219.

[8] G. V. Torrico Bascop and I. Barbi, Generation of a Family of Non-Isolated DC-DC PWM Converters Using New Three-State Switching Cells, in IEEE Power Eletronic Specialists Conference, 2000, pp. 858-863.

[9] D'Errico, L.; Lidozzi, A. and Solero, L., Neutral point clamped converter for high fundamental frequency applications, in IET Power Electronics, 2011, pp. 296 308, Vol. 4.

[10] M. H. Kheraluwala, R. W. Gascoigne, D. M. Divan, E. D. Baumann, Performance characterization of a high-power dual active bridge dc-dc converter, IEEE Trans. Power Electron., vol. 28, n. 6, pp. 12941301, Nov.-Dec. 1992.

[11] L. C. S. Mazza, D. S. Oliveira, F. L. M. Antunes, D. B. S. Alves and J. J. S. Souza, "A soft switching bidirectional DC-DC converter with high frequency isolation," 2015 IEEE 13th Brazilian Power Electronics Conference and 1st Southern Power Electronics Conference (COBEP/SPEC), Fortaleza, 2015, pp. 1-6.

[12] Hatua, K.; Dutta, S.; Tripathi, A.; Seunghun Baek; Karimi, G.; Bhattacharya, S., "Transformer less Intelligent Power Substation design with 15kV SiC IGBT for grid interconnection," Energy Conversion Congress and Exposition (ECCE), 2011 IEEE , vol., no., pp.4225,4232, 17-22 Sept. 2011.

[13] Kadavelugu, A.; Mainali, K.; Patel, D.; Madhusoodhanan, S.; Tripathi, A.; Hatua, K.; Bhattacharya, S.; Ryu, S.-H.; Grider, D.; Leslie, S., "Medium voltage power converter design and demonstration using 15 kV SiC N-IGBTs," Applied Power Electronics Conference and Exposition (APEC), 2015 IEEE , vol., no., pp.1396,1403, 15-19 March 2015.

[14] Madhusoodhanan, S.; Bhattacharya, S.; Hatua, K., "A unified control scheme for harmonic elimination in the front end converter of a 13.8 kV, 100 kVA transformerless intelligent power substation grid tied with LCL filter," Applied Power Electronics Conference and Exposition (APEC), 2014 Twenty-Ninth Annual IEEE , vol., no., pp.964,971, 16-20 March 2014.

[15] Tripathi, A.; Mainali, K.; Patel, D.; Kadavelugu, A.; Hazra, S.; Bhattacharya, S.; Hatua, K., "Design considerations of a 15kV SiC IGBT enabled high-frequency isolated DC-DC converter," Power Electronics Conference (IPEC-Hiroshima 2014 - ECCE-ASIA), 2014 International , vol., no., pp.758,765, 18-21 May 2014.

[16] Tripathi, A.K.; Hatua, K.; Bhattacharya, S., "A comparative study of three-phase dual active bridge topologies and their suitability for D-Q mode control," Energy Conversion Congress and Exposition (ECCE), 2012 IEEE , vol., no., pp.1719,1724, 15-20 Sept. 2012.